

# Analysis and Optimization of Rotor-twisted Structure for 12/10 Alternate Poles Wound FSPM Machine for Electric Vehicles

De'e Xie \*, Yu Wang \*\*, and Zhiqian Deng\*\*\*

**Abstract** –Fault-tolerant capability, wide speed range and overload capability are required in electric motors used in electric vehicles. In this paper, based on the analysis of the all poles wound and alternate poles wound flux-switching permanent-magnet machines, an optimization method is studied to reduce torque ripple. The method takes account of both flux-leakage and cogging torque. The simulation result shows that the method can reduce the torque ripple effectively. This study lays the foundation for the further application of FSPM in electric vehicles.

**Keywords:** Flux-weakening capability, Overload capability, Torque ripple, Optimization, Twist

## 1. Introduction

Electric vehicles become popular since they exhibit zero emission and are powered by chemical accumulators or fuel cells. With the development of electric vehicles, the choice of the electric motors most suited to this application is still a matter of discussions [1]. As a key technology for electric vehicles, motors used in electric vehicles shall meet the following requirements [2]-[5]:

- (1) Wide speed range;
- (2) Overload capability;
- (3) Fault-tolerant capability;

Induction motor and switched reluctance motor(SRM) are widely used in electric vehicles because of low cost, ruggedness and high flux-weakening capability, while torque density and efficiency of permanent magnet motor are superior to induction motor and SRM [6]-[7].

Flux-switching permanent-magnet motor (FSPM) is a recently emerged novel brushless machine having magnets in the stator with doubly-salient structure [8]. Its appearance provides a new idea for study of high-performance motor suited to electric vehicles and attracts considerable interest of scholars at home and abroad [9]-

[19]. Compared with the traditional rotor-PM machine, the FSPM machine exhibits the following advantages [8]-[21]:

- (1) Simple and robust structure;
- (2) Easily managing temperature rise of magnets on the stator;
- (3) The PM field and the armature field are in parallel, hence the armature field has little influence on the PM.

Electromagnetic performance of FSPM machine is studied in [9]. Because of complementary coils, conventional FSPM machine has sinusoidal back-EMF waveform. The concept of alternate teeth wound fractional-slot PM machines is extended to the FSPM machines by employing alternate poles wound. The isolated coils in each slot minimize the coupling between phases and increase the potential to fulfill the requirements for a machine to be fault tolerant [14]-[15], and it has a very similar overload capability to the conventional machine [14]. However, this is achieved with a larger torque ripple due to the presence of significant harmonics in the back-EMF waveform [15]. To reduce the consumption of PM, the multi-tooth, C-core, and E-core FSPM machines are developed but without compromising the torque capability [16]-[19], the flux-weakening capability of the multi-tooth, E-core and C-core SFPM machine are infinite and much higher than the conventional FSPM machine [18].

In order to obtain an electric motor suited to electric vehicles, this paper analyzes the potential of the overload capability of C-core, and presents an optimization method of axial with twisted-rotor to reduce the torque ripple of alternate poles wound FSPM machine.

\* College of automation engineering, Nanjing University of Aeronautics and Astronautics, Nanjing, China. (1013807715@qq.com)

\*\* College of automation engineering, PHD, lecturer, Nanjing University of Aeronautics and Astronautics, Nanjing, China. (49164267@qq.com)

\*\*\* College of automation engineering, Professor, Nanjing University of Aeronautics and Astronautics Nanjing, China. (dzq@nuaa.edu.cn)

Received 13 June 2013; Accepted 19 August 2013

This paper is organized as follows. Section 2 gives the analysis on potential of existing topologies in the case of C-core FSPM machine, the torque capability and flux-weakening capability of alternate poles wound FSPM machine are also discussed in Section 2. The optimization method is studied in Section 3. Section 4 gives the results of finite element analysis after optimization. And finally, conclusions are given in Section 5.

## 2. Potential of existing topologies

### 2.1 C-core FSPM machine

The multi-tooth, C-core and E-core FSPM machine reduce the magnet usage by a half relative to the conventional FSPM machines, as shown in Fig. 1. However, they show a marked reduction in overload capability. In the case of C-core FSPM machine, Fig. 2 shows the variation in the average torque with electric loading for C-core FSPM machine. It is shown that C-core FSPM machine exhibits a higher torque density at relatively low currents in area I, while it is the opposite when the current density increases

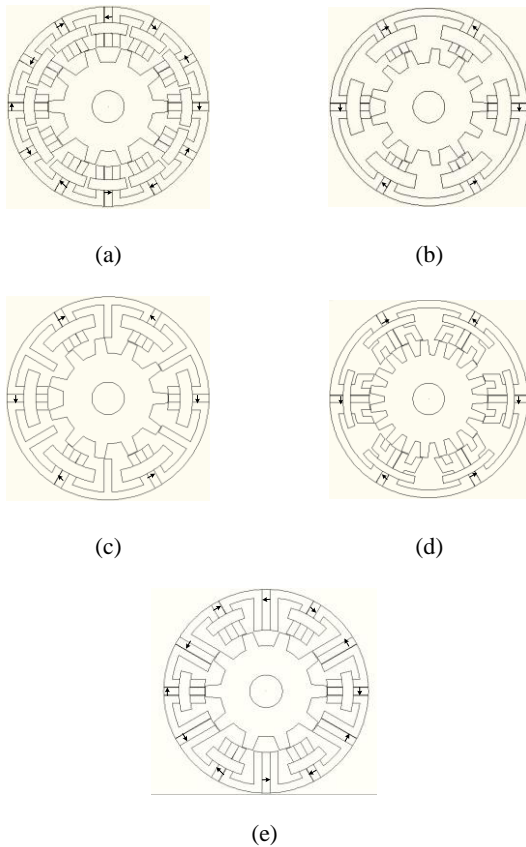


**Fig. 1.** Machine topologies. (a) Conventional. (b) C-core. (c) E-core. (d) Multi-tooth. (e) Alternate poles wound.

in area II, Fig. 2. The torque capability can be improved by increasing the consumption of PM, such as Ccore-2. However, it cannot be improved indefinitely even if increasing the width of stator teeth, rotor teeth and yoke simultaneously since inductance of C-core FSPM machine is much larger than the conventional machine, armature reaction saturates more quickly.

### 2.2 Alternate poles wound FSPM machine

Fig. 3 shows the torque-current and torque-position characteristics of alternate poles wound FSPM machine. It can be seen that alternate poles wound FSPM machine competes favorably with the conventional machine in terms of torque capability, but the torque ripple is larger, nearly twice the value of conventional machine. Torque-speed characteristics of these two topologies are compared in

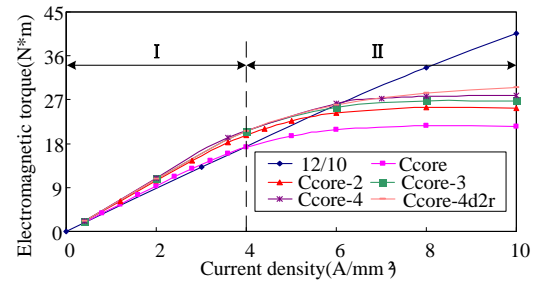


**Fig. 2.** Torque-current characteristics of C-core

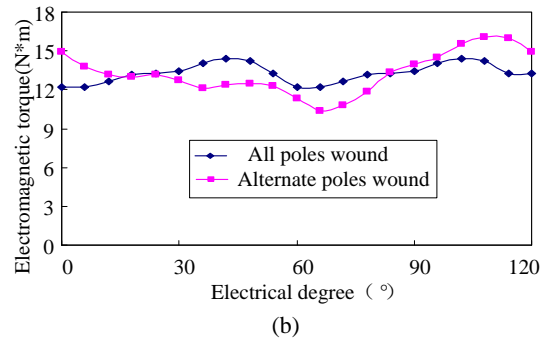
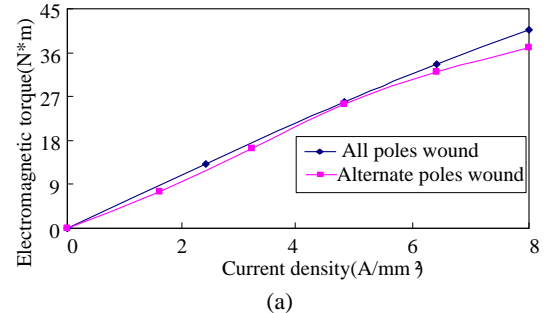


**Fig. 3.** Torque-current and torque-position characteristics of alternate poles wound FSPM machine. (a) Torque-current characteristic. (b) Torque-position

Fig. 4. As will be seen, a significant difference occurs in the torque-speed curves between the conventional and alternate poles wound FSPM machine. The flux weakening capability of the alternate poles wound FSPM machine is much higher than the conventional FSPM machine.

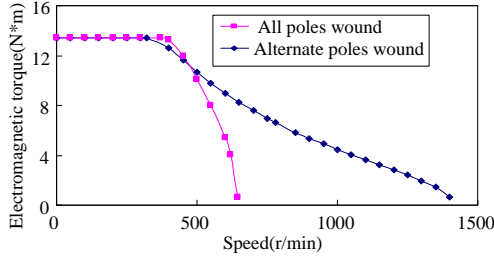


Fig. 4. Torque-speed characteristic of alternate poles wound machine.

### 3. An optimization method

In order to reduce torque ripple, this section presents an optimization method with compromising both flux-leakage and cogging torque, Fig. 5.

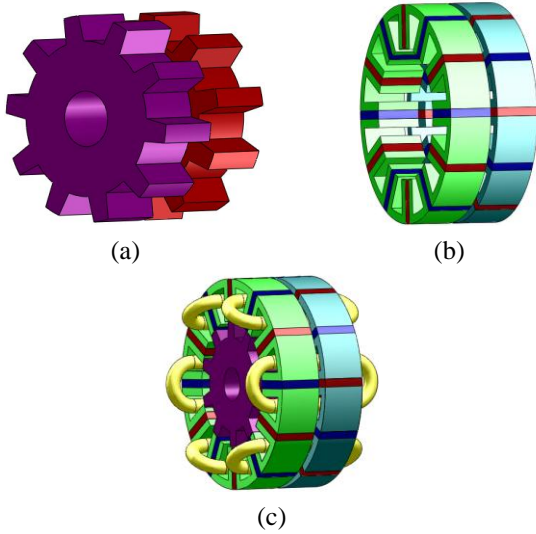


Fig. 5 Alternate poles wound FSPM machine. (a) Configuration of the rotor. (b) Configuration of the stator. (c) Configuration of the machine.

#### 3.1 Flux-leakage

The flux-leakages of two parts of FSPM machine are given by

$$\psi_I = \Psi_1 \sin(\omega t + \varphi_1) + \Psi_2 \sin(2\omega t + \varphi_2) \quad (1)$$

$$\psi_{II} = \Psi_1 \sin(\omega t + \varphi_1 + \alpha_s) + \Psi_2 \sin(2\omega t + \varphi_2 + 2\alpha_s) \quad (2)$$

where,  $\psi_I$  and  $\psi_{II}$  are the flux-leakages of the two parts of the motor, respectively.  $\Psi_1$  and  $\Psi_2$  are the amplitudes of the fundamental and second-order harmonic flux-leakage, respectively.  $\omega$  is the electrical rotor speed,  $\varphi_1$  and  $\varphi_2$  are the phases of the fundamental and second-order harmonic flux-leakage, respectively.  $\alpha_s$  is the stagger electric degree between the two parts of the rotor.

Thus,

$$\begin{aligned} \psi &= \psi_I - \psi_{II} \\ &= -2(\Psi_1 \sin \frac{\alpha_s}{2} \cos(\omega t + \varphi_1 + \frac{\alpha_s}{2}) + \Psi_2 \sin \alpha_s \cos(2\omega t + \varphi_2 + \alpha_s)) \end{aligned} \quad (3)$$

where,  $\psi$  is the flux-leakage of the motor.  $2\Psi_1 \sin(\alpha_s/2)$  is the amplitude of fundamental.

$$k = (2\Psi_2 \cos \frac{\alpha_s}{2}) / \Psi_1 \quad (4)$$

where,  $k$  is defined as the amplitudes of the second-order harmonic flux-leakage relative to the amplitude of fundamental.  $k=0$  means FSPM machine exhibits symmetrical flux-leakage waveform [22], Fig. 6.

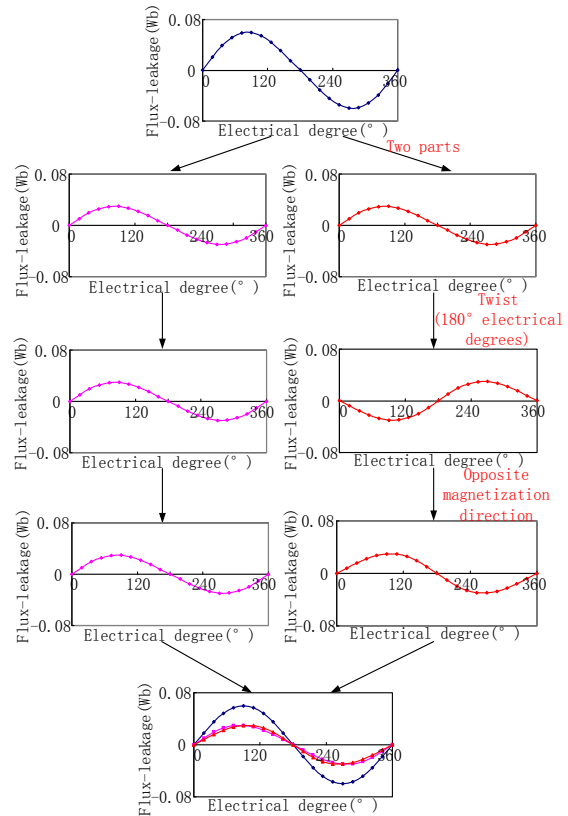


Fig. 6. Diagram of reducing the flux-linkages asymmetry by the twisted-rotor

### 3.2 Cogging torque

Import data of finite element analysis into MATLAB to use Fourier decomposition. Based on the result of Fourier decomposition, the cogging torque of the FSPM motor is given by (5), (6).

$$T_{\text{cogI}} = T_{\text{cm1}} \sin(6\omega t + \varphi_{\text{cog1}}) + T_{\text{cm2}} \sin(12\omega t + \varphi_{\text{cog2}}) \quad (5)$$

$$T_{\text{cogII}} = T_{\text{cm1}} \sin(6\omega t + \varphi_{\text{cog1}} + 6\alpha_s) + T_{\text{cm2}} \sin(12\omega t + \varphi_{\text{cog2}} + 12\alpha_s) \quad (6)$$

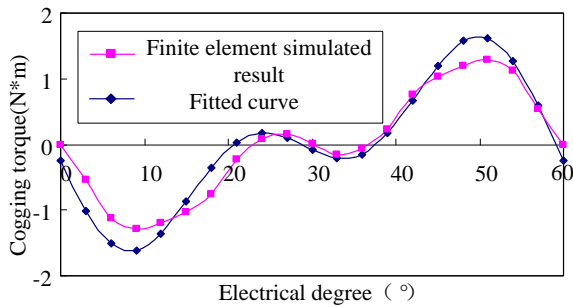
where,  $T_{\text{cogI}}$  and  $T_{\text{cogII}}$  are cogging torques of the two parts of the motor, respectively,  $T_{\text{cm1}}$  and  $T_{\text{cm2}}$  are the magnitudes of the fundamental and the second-order harmonic component of cogging torque, equal to 0.52 and 0.42 N\*m, respectively.  $\varphi_{\text{cog1}}$  and  $\varphi_{\text{cog2}}$  are the phase angles of the fundamental and the second-order harmonics component of cogging torque, equal to 184.5 and 191.4, respectively.

Thus,

$$T_{\text{cog}} = T_{\text{cogI}} + T_{\text{cogII}} \quad (7)$$

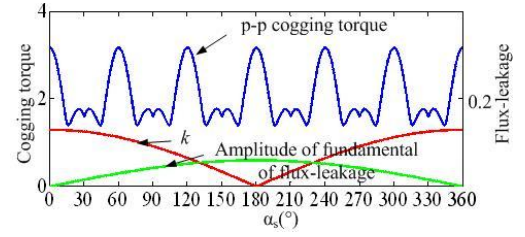
where,  $T_{\text{cog}}$  is the cogging torque of alternate poles wound FSPM machine.

Fig. 7 shows the finite element simulated result and fitted curve of cogging torque. It shows that the two curves are basically the same.



**Fig. 7.** The finite element simulated result and fitted curve of cogging torque

Fig. 8 shows the variation in the amplitude of fundamental of flux-leakage,  $k$  and p-p cogging torque with  $\alpha_s$ . It can be found that when  $\alpha_s=180^\circ$ , the maximum amplitude of fundamental of flux-leakage and the minimum  $k$  is obtained, however, the p-p cogging torque is the maximum. When  $\alpha_s=198^\circ$ , the p-p cogging torque is the minimum, the amplitude of fundamental of flux-leakage is a little smaller and  $k$  is slightly larger compared to  $\alpha_s=180^\circ$ , respectively.



**Fig. 8.** Variation in the amplitude of fundamental of flux-leakage,  $k$  and p-p cogging torque with  $\alpha_s$ .

## 4. Comparison and validation

### 4.1 Flux-leakage

Fig. 9 shows the flux-leakage of alternate poles wound FSPM machine. It is shown that it exhibits asymmetrical flux-leakage, as reported in [14]. When  $\alpha_s=180^\circ$ , the flux-leakage shows symmetrical waveform since coils of two parts of motor are complementary. When  $\alpha_s=195^\circ$  and  $\alpha_s=198^\circ$ , the machine has similar fundamental flux-leakage with that when  $\alpha_s=180^\circ$ .

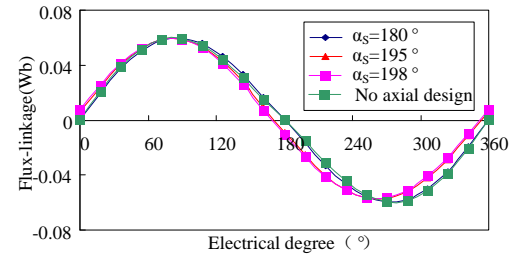


**Fig. 9.** Flux-leakage of alternate poles wound FSPM machine.

### 4.2 Cogging torque

Fig. 10 shows the cogging torque of alternate poles wound FSPM machine. It can be found that when  $\alpha_s=180^\circ$ , the cogging torque is the same as that when there is no axial design since the electric period of cogging torque is  $60^\circ$ . When  $\alpha_s=195^\circ$  and  $\alpha_s=198^\circ$ , the FSPM machine exhibits 50% smaller p-p cogging torque than that when  $\alpha_s=180^\circ$ .

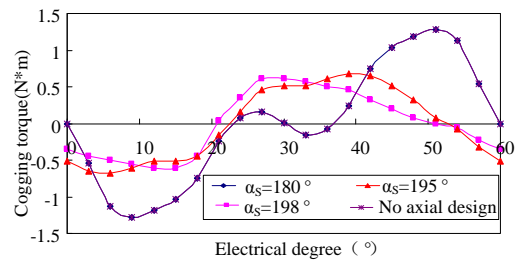
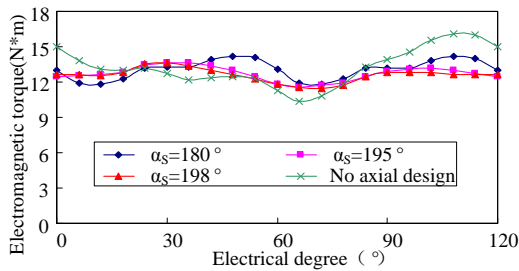


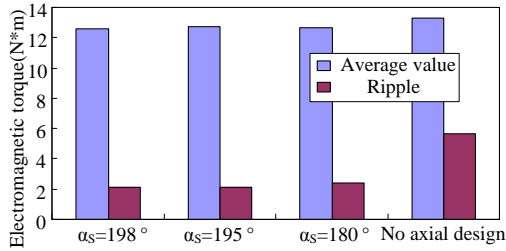
**Fig. 10.** Cogging torque of alternate poles wound FSPM machine.

### 4.3 Electromagnetic torque

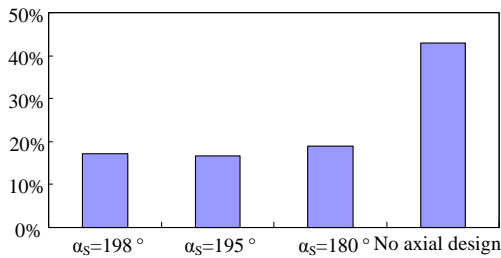
The variation of electromagnetic torque with rotor position at rated current is shown in Fig. 11 (a). In Fig. 11 (b), it can be seen that when there is no axial design, the alternate poles wound FSPM machine exhibits the maximum average torque. However, the torque ripple is 50% larger than that when  $\alpha_s=180^\circ, 195^\circ, 198^\circ$ . Fig. 11 (c) shows the relative torque ripple. It is shown that the minimum torque ripple is obtained when  $\alpha_s=195^\circ$ , about 40% of that when there is no axial design and 85% of that when  $\alpha_s=180^\circ$ , respectively.



(a)



(b)



(c)

**Fig. 11.** Electromagnetic torque of alternate poles wound FSPM machine. (a) Electromagnetic torque. (b) Average torque and torque ripple. (c) Relative torque ripple.

### 4.4 Torque-current and torque-speed characteristics

Figs.12 and 13 show the torque-current and torque-speed characteristics of alternate poles wound FSPM machine, respectively. It can be found that no matter before or after optimization, the curves are almost the same. The optimization method does not affect the torque-current and torque-speed characteristics.

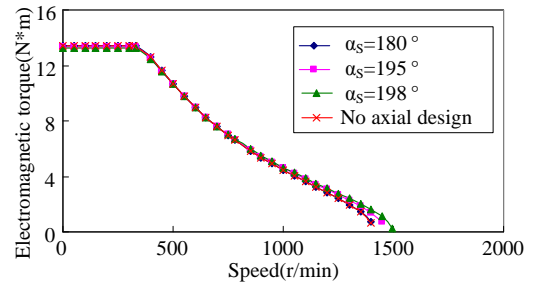


**Fig. 12.** Torque-current characteristic

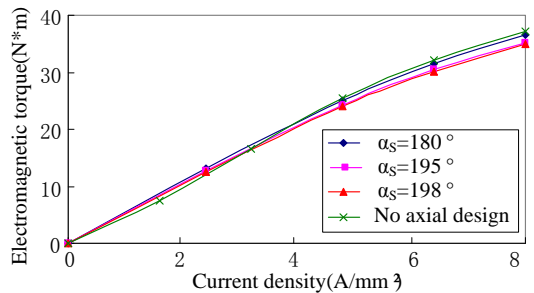


**Fig. 13.** Torque-speed characteristic

## 5. Conclusion

Flux-switching permanent-magnet motor has magnets in the stator with doubly-salient structure. This paper analyses the potential of existing FSPM machine topologies for application in electric vehicles and proposes an optimization method of axial with twisted-rotor to reduce torque ripple of alternate poles wound FSPM machine.

- (1) Multi-tooth, C-core and E-core FSPM machines reduce the magnet usage by a half relative to the conventional FSPM machines. However, the overload capability is low and cannot be improved effectively even with increasing the cost of PM.
- (2) Alternate poles wound FSPM machine exhibits high torque capability and flux-weakening capability. However, it has asymmetric back-EMF and high torque ripple.
- (3) Under the premise of maintaining overload and flux-weakening capability, this paper presents an optimization method to reduce torque ripple with compromising both back-EMF and cogging torque.

## Acknowledgements

This work was supported by the Research Fund for the Doctoral Program of Higher Education of China under Project 2011321813000 and Postdoctoral Science Foundation of Jiangsu province under Project 1301007B.

## References

- [1] El-Refae, A. M., "Motors/generators for traction/propulsion applications: a review," *IEEE Vehicular Technology Magazine*, vol. 8, pp.90-99, Mar. 2013.
- [2] Yang Liu, Jin Zhao and Rui Wang, "Performance improvement of induction motor current controllers in field-weakening region for electric vehicles," *IEEE Transactions on Power Electronics*, vol. 28, pp. 2468-2482, May. 2013.
- [3] Peter Pišek, Bojan Štumberger and TineMarčič, "Design analysis and experimental validation of a double rotor synchronous PM machine used for HEV," *IEEE Transactions on Magnetics*, vol. 49, pp. 152-155, Jan. 2013.
- [4] Peter Sergeant and Alex Van den Bossche, "Influence of the amount of permanent magnet material in fractional-slot permanent magnet synchronous machines," *IEEE Transactions on Industrial Electronics*, vol. pp. 1, Apr. 2013.
- [5] Gianmario Pellegrino and Alfredo Vagati, "Performance comparison between surface-mounted and interior PM motor drives for electric vehicle application," *IEEE Transactions on Industrial Electronics*, vol. 59, pp. 803-811, May. 2011.
- [6] Terras,J.M., Neves, A, and Sousa,D.M, "Estimation of the induction motor Parameters of an electric vehicle," *Vehicle Power and Propulsion Conference*, pp. 1-6, Sept. 2010.
- [7] Shimura,H. and Nakamura,T, "Calculated characteristics of HTS induction/synchronous machine below and above its critical temperature," *IEEE Transactions on Applied Superconductivity*. vol. 23, Jun. 2011.
- [8] E. Hoang, "Switching flux permanent magnet polyphased synchronous machines," *The 7th European Conference on Power Electronic and Applications*, 1997.
- [9] Z Q Zhu, Y Pang, and S Iwasaki, "Analysis of electromagnetic performance of flux-switching permanent-magnet machines by nonlinear adaptive lumped parameter magnetic circuit model," *IEEE Transactions on Magnetics*, vol. 41, pp. 4277-4287, Nov. 2005.
- [10] Wang,C.F. and Shen,J.X., "A method to segregate detent force components in permanent-magnet flux-switching linear machines," *IEEE Transactions on Magnetics*, vol. 48, pp. 1948-1955, May. 2012.
- [11] Weizhong Fei, Luk,P.C.K, and Jian Xin Shen, "Permanent-magnet flux-switching integrated starter generator with different rotor configurations for cogging torque and torque ripple mitigations," *IEEE Transactions on Industry Applications*, vol. 47, pp.1247-1256, May-June. 2011.
- [12] Huang,L. and Yu,H., "Study on a long primary flux-switching permanent magnet linear motor for electromagnetic launch systems," *IEEE Transactions on Plasma Science*, vol. 41, pp. 1138-1144, May. 2013.
- [13] Tsarafidy Raminosa and Chris Gerada, "Design considerations for a fault-tolerant flux-switching permanent-magnet machine," *IEEE Transactions on Industrial Electronics*, vol. 58, pp. 2818-2825, Jul. 2011.
- [14] J.T.Chen and Z.Q.Zhu, "Comparison of all and alternate poles wound flux-switching pm machines having different stator and rotor pole numbers," *IEEE Transactions on Industry Applications*, vol. 46, pp.1406-1415, Jul.-Aug. 2010.
- [15] Richard L.Owen, and Z.Q.Zhu, "Alternate poles wound flux-switching permanent-magnet brushless AC machines," *IEEE Transactions on Industry Applications*, vol. 46, pp. 790-797, Mar.-Apr. 2010.
- [16] Z Q Zhu and J T Chen, "Analysis of a novel multi-tooth flux-switching PM brushless AC machine for high torque direct-drive applications," *IEEE Transactions on Magnetics*, vol. 44, pp. 4313-4316, Nov. 2008.
- [17] J T Chen, Z Q Zhu, and S Iwasaki, "A novel E-core flux-switching PM brushless AC machine," *Energy Conversion Congress and Exposition (ECCE)*, pp. 3811-3818, Sept. 2010.
- [18] Zhu,Z.Q., AL-Ani, and M.M.J., "Comparative study of torque-speed characteristics of alternate switched-flux permanent magnet machine topologies," *International Conference on Power Electronics, machine and drives*, pp. 1-6, Mar. 2012.
- [19] J.T.Chen and Z.Q.Zhu, "Comparison of losses and efficiency in alternate flux-switching permanent magnet machines," *International Conference on Electrical Machines*, pp. 1-6 Sept. 2010.
- [20] Zheng,Ping, "Magnetic characteristics investigation of an axial-axial flux compound-structure PMSM used for HEVs," *IEEE/ASME Transactions on Magnetics*, vol. 46, pp. 2191-2194, Jun. 2010.
- [21] Reigosa and David Diaz, "Temperature issues in saliency-tracking based sensorless methods for PM synchronous machines," *IEEE Transactions on Industry Applications*, vol. 47, pp. 1352-1360, May-Jun. 2011.
- [22] Yu Wang and Zhiquan Deng, "A multi-tooth fault-tolerant flux-switching permanent-magnet machine with twisted-rotor," *IEEE Transactions on Magnetics*, vol. 48, pp. 2674-2684, Oct. 2012.



**De'e Xie** received B.S degree in electrical engineering from Nanjing University of Aeronautics and Astronautics, Nanjing, China, in 2012. She is currently working toward the M.Sc. degree in the Department of Electrical Engineering, Nanjing University of Aeronautics and Astronautics.

Her research interests include flux-switching machines.



**Yu Wang** received Ph.D. degree in electrical engineering from Nanjing University of Aeronautics and Astronautics, Nanjing, China, in 2013. He is the holder of ten China Invention Patents. His research interests include design and control of flux-switching machines.



**Zhiquan Deng** received Ph.D. degree in engineering machinery from Northeastern University, China, in 1996. In 1996, he was a Postdoctoral Fellow with the Nanjing University of Aeronautics and Astronautics, Nanjing, China, where he joined the

Department of Electrical Engineering in 1998 and is currently a Professor with the College of Automation Engineering. His current research interests include bearingless motor drive systems, magnetic bearings, super high-speed electrical machines, and flux-switching machines.